Targeted immunosuppression enhances repeated gene delivery

Maria Chen
Rice University
Boram Kim
Rice University
Maria Jarvis
Rice University
Samantha Fleury
Rice University
Shuyun Deng
Rice University
Shirin Nouraein
Rice University
Susan Butler
Rice University https://orcid.org/0000-0002-7116-7516
Sangin lee
Rice University
Courtney Chambers
Baylor college of medicine
H. Courtney Hodges
Baylor college of medicine
Jerzey Szablowski
Rice University
Junghae Suh
Omid Veiseh (omid.veiseh@rice.edu)
Rice University https://orcid.org/0000-0003-1153-8079

Article

Keywords: Adeno-associated viruses, vectors, gene delivery, immunotherapy, Blood-brain barrier, brain delivery, immunogenicity

Posted Date: March 1st, 2022

DOI: https://doi.org/10.21203/rs.3.rs-1382849/v1

Additional Declarations: Yes there is potential conflict of interest. J.S. is an employee of Biogen Inc. as of 2019. O.V. is a member of the Scientific Advisory Board of Sigilon Therapeutics and holds equity in the Avenge Bio and Pana Bio.

Version of Record: A version of this preprint was published at Gene Therapy on November 14th, 2022. See the published version at https://doi.org/10.1038/s41434-022-00371-0.

Targeted immunosuppression enhances repeated gene delivery

Maria Chen*[1,2], Boram Kim*[1], Maria I. Jarvis*[1], Samantha Fleury[1], Shuyun Deng[1], Shirin Nouraein[1], Susan Butler[1], Sangsin Lee[1], Courtney Chambers[3], H. Courtney Hodges[1,4], Jerzy O. Szablowski[1,5], Junghae Suh[1,6,‡], Omid Veiseh[1,‡]

[1]Department of Bioengineering, Rice University, Houston, TX, USA

[2]Medical Scientist Training Program, Baylor College of Medicine, Houston, TX, USA

[3]Translational Biology and Molecular Medicine Graduate Program, Baylor College of Medicine, Houston, TX, USA

[4]Center for Precision Environmental Health, Department of Molecular and Cellular Biology, and Dan L Duncan Comprehensive Cancer Center, Baylor College of Medicine, Houston, TX, USA

[5]Department of BioSciences, Rice University, Houston, TX, USA

[6]Systems, Synthetic, and Physical Biology Program, Rice University, Houston, TX, USA

***Equal Contribution**

[‡]Corresponding author

E-mail address: JS <jsuh@rice.edu>, OV <omid.veiseh@rice.edu>

Abstract

Adeno-associated virus (AAV) vector-based gene therapies can be applied to a wide range of diseases. AAV expression can last for months to years, but vector re-administration may be necessary to achieve life-long treatment. Unfortunately, immune system response against these vectors is potentiated after the first administration, which prevents the clinical use of repeated administration of AAVs. Reducing immune response against AAVs while minimizing immunosuppression would improve gene delivery efficiency and long-term safety. In this study, we quantified the contributions of multiple immune system components towards AAV response in mice. We identified B-cell-mediated immunity as a critical component preventing vector re-administration. Specifically, we found that IgG depletion was insufficient to enhance re-administration, suggesting the key role of B-cell mediated IgM antibodies in the immune response against AAV. Further, we also found that AAV-mediated transduction is improved compared to wild-type mice in μMT mice that lack functional IgM heavy chains and cannot form mature B-cells. Combined, our results suggest that IgM production in B cells is a potential target for therapeutics enabling AAV re-administration. Our results also suggest that the μMT mice are a potentially useful experimental model for gene delivery studies since they allow for up to 15-fold more efficient gene delivery.

Keywords:

Adeno-associated viruses, vectors, gene delivery, immunotherapy, Blood-brain barrier, brain delivery, immunogenicity

Introduction

The U.S. Food and Drug Administration has recently approved multiple adeno-associated virus (AAV) based gene therapies for use in humans[1]. These approvals, along with developments in AAV research and successes in numerous clinical trials, have marked AAV as a leading vector in the field of gene therapy[2]. Despite these successes, however, the host immune response against the vector capsid is a major barrier to achieving therapeutic efficacy in patients who have previously been exposed to AAV[3]. Current clinical trials screen for neutralizing antibodies (NAb) against AAV and exclude patients with NAbs above a set threshold. However, 20-80% of the population worldwide carry NAbs to existing AAV serotypes[4-10]. To combat this, new AAV variants are being developed to evade pre-existing antibodies[11-13]. Nevertheless, pre-clinical and clinical studies[11,14-16] show that regardless of the origin of the AAV capsid, a single administration generates persistent anti-AAV NAbs, which would abolish any benefit of subsequent AAV re-administrations for an effective therapeutic response[17-19].

The ability to re-administer gene therapy is vital for achieving long-lasting therapeutic efficacy. Because the AAV genome is mainly non-integrating[20-22], loss of transgene expression can occur over time due to dilution of viral transgenes as transduced cells replicate[23,24]. Loss of transgene expression may be particularly relevant in treating life-long genetic disorders, e.g., pediatric populations. In pediatric patients, a high level of tissue proliferation and organ growth will lead to the dilution of non-integrating vectors, such as AAV through the cell division. Furthermore, recent clinical studies suggest AAV-mediated gene expression declines over time. In a long-term follow-up of clinical trial participants, BioMarin Phase 1/2 study of valoctocogene roxaparvovec for treating severe hemophilia A showed that transgene production in patients had

continually decreased over several years (NCT02576795)[25]. For patients with lifelong genetic disorders, such a decrease could reduce the concentration of gene products outside the therapeutic window. On the other hand, simply increasing the dose of AAV at the first administration may lead to vector toxicity[26], an immune response against both vector[27] and transgene[28], and potentially the side effects from overexpression of the transgene[29].

Extensive studies in animal models and clinical trials have contributed to our fundamental understanding of the immune response against AAV[30]. Initial studies emphasized the adaptive immune system since AAV induces a mild innate response compared to other viruses[31]. However, there is emerging evidence that the innate immune system plays an essential role in priming effector responses[32]. Upon administration, AAVs are taken up by antigen-presenting cells (APCs) and detected by pattern recognition receptors (PRRs). Toll-like receptor 9 (TLR9) has been implicated in CD8+ T cell responses and type I IFN production, while its downstream adaptor MyD88 may also contribute to B cell responses. Both TLR9 and MyD88 knockout mice experienced decreased T cell activation and antibody production, though these responses may be serotype-specific[33-36]. The virus capsid may also interact with the complement system leading to increased capsid uptake and activation of macrophages *in vitro* and decreased anti-AAV antibody production in a C3 knockout mouse line[37]. Mobilization of APCs ultimately leads to priming of the adaptive immune system, with the presentation of capsid-derived epitopes via major histocompatibility complex (MHC) class II and class I, activating CD4+ and CD8+ cells and leading to humoral and cell-mediated immune responses[38-41].

Currently, there is no standard targeted approach for suppressing the immune response against AAVs. Strategies such as serotype switching[42,43], local vector delivery[44], temporary immunosuppression[45,46], apheresis[47,48], and immune cell depletion[49] have all achieved various

levels of success. Various immune suppression regimens are also being studied, including the co-administration of rapamycin nanoparticles to modulate the anti-AAV immune response[18]. These methods are promising, but immunosuppression can lead to various side effects, such as an increased risk of infection and cancer[50]. Thus, it is desirable to find the most targeted regimen that would allow repeated AAV therapy.

While many components of the immune system have been identified and studied as potential targets for immunosuppression, their relative contribution to the general immune response remains mostly unexplored. Here we examine the roles of innate and adaptive immunity on the host response against the AAV capsid in mice. We used a panel of immune-deficient mouse models and cell-depletion strategies to measure the vector efficacy and immune response after systemic administration and re-administration of AAV serotype 9 (AAV9). One challenge in comparing the results of different past studies is the variability in factors such as virus production methods, cell culture conditions, experimental protocols, and assays standards. We aim to minimize these variabilities in our study by performing all experiments in the same facility, thus allowing us to compare better the relative importance of various immune components in the overall anti-AAV immune response.

Using a panel of mice bred from a similar genetic background (C57BL/7 background) but varying immunology phenotypes, we can infer the relative importance of the various immune system components. Our panel included mice deficient in macrophages, C3 complement, TLR9, MyD88, IL15 signaling, T cells, and B cells. Two strains of particular interest in our panel are the μMT (B6.129S2-Ighm^{tm1Cgn}/J) and R2G2 (B6;129-Rag2^{tm1Fwa}IL2rgt^{m1Rsky}/DwlHsd) mice. The μMT mice lack functional IgM heavy chains and cannot form mature B cells[51]. IgM is an early antibody isotype formed in response to foreign antibodies. Further B cell interaction with other

immune signals, such as cytokines or interactions with T cells, can result in class-switch recombination that produces different immunoglobulin isotypes[52]. Immunoglobulin production can undergo isotype switching from IgM to IgG, which is long-lasting and is the most abundant antibody isotype in the blood. The R2G2 mouse is an ultra-immunodeficient animal model with knockout mutations in the *IL2RG* and *Rag2*, with deficiencies in T cells, B cells, NK cells, dendritic cells, macrophages, neutrophils, and receptors for a variety of cytokines[53].

Here, we identified the most crucial immune cell populations for successful intravenous re-administration of AAV9. We further characterized the anti-AAV IgM, IgG, and neutralizing antibody profiles in wild-type mice and a panel of immune-compromised mice after single and double AAV injection. Additionally, we created an immune-depleted mouse model that highlighted the importance of complete antibody elimination for re-administration of AAV. Finally, we established the use of μMT mice as a model for gene deliveries. Overall, our findings will contribute to developing strategies for AAV gene therapies to overcome the barrier posed by the host immune system.

Materials and Methods

Plasmids

Transgene plasmids were recombinant AAV vector packaging single-stranded reporter genes under the CAG promoter with a WPRE element. The vector backbone was derived from pAAV-CAG-RLUC, a gift from Mark Kay (Addgene plasmid # 83282; http://n2t.net/addgene:83282; RRID: Addgene_83282). The Metridia secreted luciferase (MLuc)

was synthesized by VectorBuilder following GenBank sequence LC175306 (nucleotides 6316 through 6975). Secreted embryonic alkaline phosphatase (SEAP) gene was derived from plasmid CMV-SEAP, a gift from Alan Cochrane (Addgene plasmid # 24595; http://n2t.net/addgene:24595; RRID: Addgene_24595). Reporter genes were cloned into the pAAV-CAG backbone via Gibson cloning. The pAAV2/9 plasmid, which encodes AAV2 *rep* and AAV9 *cap* genes, was used as the packaging plasmid. pXX6-80 was used as the helper plasmid.

Virus Production and Quantification

AAV vectors were produced in HEK293Tcells using triple transfection with the packaging plasmid (pAAV2/9), helper plasmid (pXX6-80), and a transgene plasmid as previously described in Chapter 2 of this thesis. Briefly, cells were harvested 48 hours after transfection, and the virus was extracted using iodixanol step gradient and ultracentrifugation. The virus was further concentrated and buffer exchanged into GB-PF68 buffer (50 mM Tris [pH7.6], 150 mM NaCl, 10mM $MgCl_2$, and 0.001% Pluronic F68) using 100-kDa molecular weight (MW) Amicon Ultra-15 Centrifugal Filter Units (Millipore, CAT: UFC910008). Quantitative polymerase chain reaction (qPCR) was used to measure the genomic titers of viruses as previously described[54], using SYBR green (Applied Biosystems, CAT 4309155) and primers against the CAG promoter (see **Supplementary Table. 1**). All virus was produced on-site except for the PHP.eB-GFP virus (Addgene, CAT 104061-PHPeB).

In Vitro Virus Characterization

To characterize transgene expression *in vitro*, transduction assays were performed in CHO-Lec2 cells. CHO-Lec2 cells were seeded in poly-L-lysine coated 96-well plates at 20,000 cells per

well 24 hours before the addition of the virus. The virus was added to cells at a multiplicity of infection (MOI) ranging from 312 – 10,000 viral genomes per cell in serum-free MEM-alpha media (Gibco, CAT: 12571063) containing 10% Penicillin-streptomycin (Life Technologies, CAT: 15140122). After 24 hours, media was changed to MEM-alpha media containing 10% fetal bovine serum (FBS, Atlanta Biologicals, Cat: S11150). At 48 hours, cells were harvested for the quantification of transgene products. For cells expressing MLuc, harvest was performed with 30μL of Passive Lysis Buffer (1x diluted in PBS) (Promega CAT: E1941) for 15 minutes at 37°C. Lysis was confirmed by visualization under the light microscope. 80μL of native coelenterazine (GoldBio, CAT: CZ2.5) diluted to 20 μg/mL in PBS was added to each well, and luminescence signal was measured using plate reader Tecan Infinite 200Pro, with 1000ms integration time. Cells expressing SEAP were lysed with RIPA Lysis Buffer (Thermo Scientific, CAT: 89900), heat-treated at 65°C for 30 minutes, and SEAP level was quantified using the Phospha-Light SEAP Reporter Gene Assay (Invitrogen, CAT: T1015).

Mice

Animal work was performed in accordance with NIH guidelines and as approved by the Rice University's Institutional Animal Care and Use Committee. Mice strains used in this study are listed in **Fig. 1B**. All animals were aged 6-12 weeks at the time of the first treatment. Viruses were administered to animals via intravenously tail-vein injections, with 1.0e11 viral genomes in 100uL volume injected for each treatment unless otherwise noted. For brain re-administration study, μMT mice were used as a model to deliver PHP.eB AAV packed with GFP. μMT and WT mice were injected with a single high dose (4.5e9 VP/g), single low dose (1.5e9 VP/g), or three weekly repeated low doses (1.5e9 VP/g) of PHP.eB AAV. Blood was collected via the saphenous

vein or in a terminal cardiac puncture procedure. Serum was obtained after allowing whole blood to coagulate at room temperature for at least 30 minutes, followed by centrifugation at 1,000xg for 10 minutes. At the termination of each experiment, mice organs were snap-frozen and stored at -80° C.

Immune Depletion in Mice

Clodrosome (Encapsula NanoSciences, CAT: CLD-8909) was used to deplete macrophages in C57BL/6 mice. 200uL of the 18.4mM clodrosome formulation was administered via intraperitoneal injection 3 days before virus injections. Clodrosome treatments were repeated weekly for the duration of the experiment, with an additional treatment given on the day of virus injections.

To deplete B- and T-cells, an antibody cocktail was administered intraperitoneally in 500uL volume to C57BL/6 mice. The cocktail contained 100ug of anti-CD3ε (BioXCell, CAT: BE0001-1), 500ug of anti-CD40L (BioXCell, CAT: BE0017-1), 250ug of anti-CD20 (BioXCell, CAT: BE0302), 250ug anti-CD19 (BioXCell, CAT: BE0150), and 250ug anti-B220 (BioXCell, BE0067). The antibody cocktails were administered 1 week before the first virus injection and continued weekly until the termination of the animals. CD19, CD20, and B220 are cell surface markers present on various stages of B cell development and are targets of depletion by anti-CD19, anti-CD20, and anti-B220. Anti-CD40L interferes with B cell activity by inhibiting B cell interaction with activated T cells. Since activity from re-administered AAV in μMT mice was only about 40% compared to singly injected mice, but 100% in R2G2 mice, we suspected that secondary factors might synergistically affect the immune response against AAV. Thus, we also included an

agent to deplete T cells, anti-CD3ε, in our antibody cocktail. Anti-CD3ε has been shown to deplete conventional T cells while sparing regulatory T cells[55].

In Vitro Neutralizing Antibody Assay

An *in vitro* neutralizing antibody assay was used to quantify the amount of anti-AAV9 neutralizing serum in mouse serum. The serum supernatant was stored at -20°C and heat-inactivated at 56°C for 30 minutes before the assay. CHO-Lec2 cells were seeded in poly-L-lysine coated white 96-well plates (Greiner Bio-One, CAT: 82050-758) at 20,000 cells/well 24 hours before the addition of the virus. MEM-alpha media containing 1% Pen-strep was used to dilute mouse serum from 1:200 to 1:102,400 by 2x serial dilution in duplicate. AAV9 virus-containing metridia luciferase transgene at 5,000 multiplicity of infection (MOI) was incubated with the various serum dilutions at 4°C for 2 hours, then added to cells. 24 hours after virus addition, media was changed to MEM-alpha media containing 1% Pen-strep and 10% fetal bovine serum (FBS). 48 hours after virus addition, media was aspirated, and cells were lysed and assayed for metridia luciferase expression as described above. Positive controls with only virus and no serum and negative controls with no virus and no serum were included with plate read. Since CHO-Lec2 cell and transduction behavior is affected by the amount of serum present, dilution curves were also generated with serum from strain-matched untreated mice and used to correct the effect of serum on cell behavior. The neutralizing antibody titer (NAb titer) is defined as the reciprocal of the dilution at which 50% of virus transduction is inhibited. To quantify the NAb titer, the transduction vs. serum dilution curves were fit using four parameters logistic regression in Prism 7 (GraphPad).

Antibody ELISA

Anti-AAV9 IgG and IgM concentrations in mouse serum were measured using enzyme-linked immunosorbent assay (ELISA). AAV9-MLuc was diluted in coating buffer (13mM Na_2CO_3 and 88mM $NaHCO_3$) and coated on 96-well Nunc Maxisorp plates (Invitrogen CAT: 44240421) at $1x10^8$ viral genomes per well. Plates were incubated overnight at 4°C, then washed three times with washing buffer (PBST: 0.05% Tween in PBS). Wells were then blocked with blocking buffer (2% BSA in PBS) for 2 hours at room temperature. Mouse serum was diluted with blocking buffer from 1:200 to 1:800,000 in duplicate and added to wells overnight at 4°C. Wells were washed three times with PBST, and the secondary antibody was added for 2 hours at 37°C. For quantification of IgG, HRP-tagged anti-mouse IgG secondary recognizing subclasses IgG1, IgG2a, IgG2b, and IgG3 (Jackson ImmunoResearch Laboratories Inc., CAT: 115-035-164) was used at 1:10,000 dilution. For quantification of IgM, HRP-tagged goat anti-mouse IgM secondary (Invitrogen, CAT: 62-6820) was used at 1:5000 dilution. To develop the signal, TMB ELISA Substrate (Abcam, CATab171522) was added to wells and incubated for 20 minutes. The reaction was terminated with 1 N HCl, and the absorbance was quantified at 450 nm using a plate reader (Tecan Infinite 200Pro). A standard curve was generated using anti-AAV9 IgG2a antibody (clone ADK8/9, American Research Products, Inc, CAT: 03-651161) for IgG quantification and purified mouse IgM (Invitrogen, CAT: MGM00) for IgM quantification.

Quantification of Transgene Expression in Serum

To quantify MLuc presence in mouse serum, serum without any heat treatment was diluted 1:20 in PBS. 20 µL of diluted serum was transferred to a white 96-well plate, 80µL of 20 µg/mL coelenterazine was added, and the luminescence was quantified on Tecan Infinite 200Pro plate reader. Serum from one mouse 6 weeks after AAV9-MLuc injection was used as positive control

and included on all plate reader runs. Relative light unit (RLU) values from each sample were normalized to positive control before comparing runs. To quantify SEAP presence in mouse serum, serum was diluted to 1:50 in Phospha-Light Reaction Buffer Diluent and heat-treated at 65°C for 30 minutes. Samples were transferred to white 96-well plates then processed according to Phospha-Light System Assay protocol (Invitrogen, CAT: T1015). Serum from one mouse 6 weeks after AAV9-SEAP injection was used as positive control and included on all plate reader runs. Relative light unit (RLU) values from each sample were normalized to positive control before comparison between runs.

DNA and RNA Extraction

Organs were harvested from mice, snap-frozen in liquid nitrogen, and stored at -80°C. The organs were thawed on ice and homogenized using Beadbug Microtube Homogenizer (Benchmark Scientific, SKU: D1030). For DNA extraction, 20mg of the homogenized organ were processed using the DNeasy Blood and Tissue Kit (Qiagen CAT: 69504). Extracted DNA was tittered using qPCR with normalization to total ng of DNA loaded. For RNA extraction, 30mg of the homogenized organ were processed using the RNeasy Mini Kit (Qiagen CAT: 74104). The extracted mRNA was converted to cDNA for RT-qPCR using the Verso cDNA Synthesis Kit with RT enhancer (Thermo Scientific, CAT: AB1453A). Both DNA and cDNA samples were diluted in sheared salmon sperm DNA to reduce noise in qPCR and RT-qPCR quantification.

Reverse Transcription qPCR

Quantitative reverse transcription-polymerase chain reaction (RT-qPCR) was used to measure gene expression in mice tissues. SYBR Green was used with appropriate primers (see

Supplementary Table. 1) and measured in the Bio-Rad C1000 thermal cycler. Primers were designed using PrimerQuest Tool (Integrated DNA Technologies).

Expression level over the housekeeping gene (β-Actin) was calculated using the $2^{-\Delta\Delta C_T}$ method, where:

$$\text{Fold change} = 2^{-\Delta\Delta C_T}$$

$$\Delta\Delta C_T = \Delta C_T(treated\ sample) - \Delta C_T(control\ sample)$$

$$\Delta C_T = C_T(gene\ of\ interest) - C_T(housekeeping\ gene)$$

Organs harvested from buffer-injected C57BL/6 mice were used as controls.

Luminex Assay

Mice spleen and liver samples were homogenized and lysed in T-PER Tissue Protein Extraction Reagent (Thermo Scientific, CAT: 78510) containing 1xHalt protease and phosphatase inhibitors (Thermo Scientific, CAT: 78445). Organ and serum samples were submitted to the Baylor College of Medicine Antibody-Based Proteomics Core for processing. The MILLIPLEX MAP Mouse Cytokine/Chemokine Magnetic Bead Panel (Millipore Sigma, CAT: MCYTMAG-70K-PX32, lot #3532037) was used to quantify the expression of 32 cytokines/chemokines. The Luminex instrument passed calibration using the Bio-Plex Calibration Kit (Bio-Rad, CAT: 171-203060) and passed validation using the Bio-Plex Validation Kit 4.0 (Bio-Rad, CAT: 171-203001). Levels below the detection limit were defined as 0 pg/mL.

Single-cell RNA-seq (scRNA-seq) analysis

C57BL/6 mice spleens from single-, double-injections and control (buffer injection) groups were homogenized and filtered with a 70μm cell strainer. Only live cells (stained with Calcein AM) were sorted using a Flow Sony MA900 Cell Sorter at a density of 1000 cells/μl in DMEM containing 10% FBS. Single-cell 5' Gene Expression Library was prepared according to Chromium NextGEM Single Cell Immune Profiling Solution 5'v2 (10x Genomics). In brief, single cells, reverse transcription (RT) reagents, Gel Beads containing barcoded oligonucleotides, and oil were loaded on a Chromium controller (10x Genomics) to generate single-cell GEMS (Gel Beads-In-Emulsions) where full-length cDNA was synthesized and barcoded for each single cell. Subsequently, the GEMS are broken, and cDNA from each single cell is pooled. Following cleanup using Dynabeads MyOne Silane Beads, cDNA is amplified by PCR. The amplified cDNA is fragmented to optimal size, and the 5' Gene Expression (GEX) library was generated via End-repair, A-tailing, Adaptor ligation, and PCR amplification. To construct the immune repertoire library, full-length V(D)J segments are enriched from amplified cDNA via PCR amplification with primers specific to the constant regions in T cells and B cells. Enzymatic fragmentation and size selection are used to generate variable length fragments that collectively span the entire transcript. Library construction was carried out via End repair, A-tailing, Adaptor ligation, and PCR amplification. The resulting libraries were sequenced on an Illumina NovaSeq 6000 flow cell. Transcripts within each cell were counted using the 10x Cell Ranger 5.0.1 pipeline, with genome mapping using STAR v2.7.2a. To identify immune cell populations, the scRNA-seq data was visualized using tSNE embedding in Loupe Browser 5.0. The resulting clusters were assessed for the expression of common immune cell marker genes and were then classified as a specific immune cell type based on their expression profiles. The cell identities of each of the clusters were resolved using the following markers: Cd3e (T cells), Cd19 (B cells), Csf1r and Fn1

(monocytes/macrophages), Flt3 (dendritic cells), Ly6g and Hdc (neutrophils), Prf1 (NK cells), and Gypa (erythrocytes). Based on these markers, individual cell barcodes were assigned to their corresponding immune cell type in the Loupe Browser. To assess changes in the infiltrate immune composition, changes of cell proportions were calculated between each AAV administration condition for each immune cell type. The significance of these changes was calculated using Fisher's exact test in R (v3.6.1), and the resulting P-values were adjusted using the Benjamini-Hochberg false-discovery rate (FDR) correction method.

FACS Analysis

Spleen, liver, and blood samples were collected from the depletion mice (weekly antibody cocktail injections) and control mice (buffer injection) after 3weeks of re-administration. Collected organs were kept in cold PBS for further processes. Organs were placed in a 6well plate with a strainer, mashed using pestles, and washed with cell staining buffer. Cells were transferred into 15ml tubes, resuspended in cell staining buffer, and centrifuged at 350g for 5mins at 4°C. Cells from organs and blood samples were resuspended in RBC lysis buffer and incubated for 10 mins at RT. Samples were centrifuged down, resuspended in cell staining buffer, and repeated the washing step one more time. Samples were resuspended in 1ml of cell staining buffer and plated into V-shaped bottom 96well plates at the density of 1 million cells per well. Plates were centrifuged at 350g for 5min and resuspended in cell staining buffer. TruStain FcX Plus buffer (with 0.25µg of anti-mouse CD16/32) was used to block Fc receptors. Cells were incubated in Fixation/Permeabilization solution for 30mins on ice for intracellular staining. Samples were centrifuged and resuspended in Perm/Wash buffer. Plates were centrifuged, resuspended with antibody cocktails, incubated in the dark for 30mins on ice. Antibody cocktails included anti-CD4,

CD5, FOXP3, CD25, CD19, CD3 and CD8. Plates were centrifuged and washed with cell staining buffer three times. Following all washing steps, samples were resuspended with FACS buffer and run through a 40μm filter for FACS analysis using a Sony MA900 Cell Sorter. Unstained and single antibody controls were also used for analysis.

Imaging and analysis

Mice brains were extracted and postfixed in 10% neutral buffered formalin (Sigma, CAT: HT501128) overnight at 4°C. The next day, brains were washed with PBS 3 times, sliced at a thickness of 50 μm using a Leica VT1200S, and stored in the dark at 4°C until mounting. VECTASHIELD Antifade mounting medium (Vector Laboratories, CAT: H-1800-10) containing 4,6-diamidino-2-phenylindole (DAPI) nuclear stain was applied to the brain sections before coverslip mounting and cured overnight in the dark at room temperature. DAPI and GFP-positive cells were imaged using the Keyence BZ-X810 fluorescence microscope. For each mouse, striatum, cortex, midbrain, and hippocampus brain regions were found, and four random areas within each region were selected and imaged. ImageJ software was used to quantify GFP positive area by first stacking the obtained TIFF images to RGB and measuring the total area above the brightness threshold of 15. The calculated GFP positive percent areas of the four images from each region were averaged to quantify an unbiased transduction efficiency of the region.

Results

Absence of B cells permits for successful AAV re-administration

We used multiple mouse strains to gauge the relative importance of numerous components of both the innate and adaptive systems. These mice were genetically modified or chemically depleted to have specific deficiencies in immune components that have been identified to play a role in the anti-AAV immune response (**Fig. 1A-B**). Before administering our vectors to animals, we first characterized vectors *in vitro* (**Supplementary Fig. 1**). We chose AAV serotype 9 (AAV9) as our vector because of its ability to transduce a variety of organs, effective liver transduction, and limited but present transduction of the central nervous system (CNS), making it applicable in a wide range of diseases[56-58]. AAV-MLuc was injected into mice, and AAV-SEAP was administered 3 weeks later (**Fig. 1C**). MLuc expression was similar in all mice groups, suggesting that these immune deficiencies did not affect the efficacy of the initial AAV injection in naïve mice (**Supplementary Fig. 2**). Mice were euthanized 6 weeks after the initial AAV treatment, and the viral DNA and transgene transcripts in their livers were quantified. Only μMT and R2G2 mice had detectable viral DNA (**Fig. 1D**), transgene mRNA (**Fig. 1E**) from AAV re-administration, showing above the threshold (dotted line) of detection. Also, SEAP expression was observed in only μMT and R2G2 mice, representing successful transduction at re-administration at week 6 (**Fig. 1F**). Re-administration of AAV in R2G2 yielded a similar protein expression level as a single injection in wild-type (WT) C57BL/6 mice (no significant measured by one-way ANOVA, WT vs. R2G2). Re-administration of AAV in μMT mice produced 44% SEAP expression compared to a single injection in WT mice. We identified B cell dysfunction as a common immune deficiency mechanism between the μMT and R2G2 mice. This result suggested that the B cells are a primary factor impeding transgene expression upon AAV re-administration.

Successful AAV re-administration requires non-detectable antibody levels

We identified B cells as crucial for the immune response against AAV, so we quantified the anti-AAV antibody profiles in mice throughout our study. We used an *in vitro* neutralization antibody (NAb) assay to measure the ability of the antibodies to neutralize AAV9 activity. In C57BL/6 mice, NAb presence was robust by one week after injection of AAV and persisted throughout this study (**Fig. 2A**). Upon AAV re-administration, there appeared to be a slight rise in NAb titer, but this increase was not statistically significant as measured by one-way ANOVA. NAbs were also tracked in the immune-deficient mouse panel (**Fig. 2B**). In the majority of the immune-deficient groups, NAb titer increased significantly at week 4 after AAV re-administration compared to week 3 *(*P<0.05* by two-way ANOVA). The values were returned to their pre-re-administration level by week 6. In the macrophage depletion and TLR9 groups, NAb titers increased after the second AAV administration to a level even higher than they did in the WT mice. MyD88 deficient mice had 9-fold lower NAb titers than the WT double injection group, but detectable titers at week 4. μMT and R2G2 mice had undetectable titers throughout the tracking period.

We quantified the presence of both IgM and IgG in the blood of WT mice using the ELISA with isotype-specific antibodies after a single (**Fig. 2C**) or double (**Fig. 2D**) AAV injection. We saw that IgM production dominated at week 1 but mostly disappeared by week 2-3. On the other hand, IgG antibodies increase over the first 2-3 weeks and are strongly present throughout the remainder of the study. IgG level, but not IgM level, increased after AAV re-administration in WT mice. IgM had robust production by week 1 in all immune-deficient mice except for μMT and R2G2 (**Fig. 2E**). IgM levels remained high over several weeks and increased after AAV re-administration in C3, MyD88, and nude mice. IgG levels increased after re-administration in all mice with a robust initial IgG response. IgG levels in MyD88, μMT, nude, and R2G2 mice were

undetectable and were significantly reduced in C3 mice (**Fig. 2F**). Taken together, SEAP expression data (**Fig. 1**) and antibody measurements (**Fig. 2**) show that AAV re-administration was only successful when IgM, IgG, and NAb levels were all below the limit of detection at the time of re-administration.

Re-administered AAV is only detectable in the spleen

We measured the biodistribution of the viruses in C57BL/6 mice to understand the distribution of virus particles after initial treatment and vector re-administration. The measurement of viral DNA provides insight on where the virus might be present, while mRNA measurements correspond to the presence of the successfully transcribed transgene. The DNA and mRNA distribution of AAV9-MLuc and AAV9-SEAP were investigated after injections into two different groups of mice separately. The values did not significantly differ at week 6 after injection ($p > 0.9$, measured by 2-way ANOVA), suggesting that transgene identity does not affect biodistribution (**Fig. 3A-B**). To obtain biodistribution for the re-administration model, we first injected AAV9-MLuc into mice, followed 3 weeks later by an injection of AAV9-SEAP into the same animals. Viral DNA and mRNA transcripts from the second administration, SEAP, were significantly decreased in all organs except for the spleen 6 weeks after the first AAV administration (**Fig. 3C-D**). Despite the presence of viral DNA and transcripts, no SEAP protein was detected in the spleen (**Supplementary Fig. 3**). The accumulation of virus capsids in the spleen of animals with anti-capsid antibodies has been previously noted in non-human privates[59]. This result suggests that, in all organs except for the spleen, the second AAV injection does not accumulate and cannot produce viral transcripts, likely due to the immune response resulting from the initial AAV administration.

AAV single administration alters a subset of the B cell population but not re-administrated AAV

Single-cell RNA-seq (scRNA-seq) can assess the composition of heterogeneous cell populations. We used scRNA-seq to evaluate the effects of AAV administration on the splenic immune cell compositions. The effects of a single or double administration of AAV were compared both to vehicle control (**Supplementary Fig. 5A**). t-SNE embedding revealed six major clusters well represented in all three treatment conditions (**Supplementary Fig. 5B**). The clusters were classified by immune population using standard cell type-specific markers. Clusters were defined as T cells, B cells, dendritic cells, macrophages (including monocytes), NK cells, neutrophils, and erythrocytes (**Fig. 4A, Supplementary Fig. 5C**). Single and double AAV injections did not significantly alter the proportions of entire immune populations present in the spleen (**Fig. 4A-B**). However, a single AAV administration did result in an enrichment of a specific B cell subset compared to both the control and double administration (**Fig. 4C-D**). A comparison of the global gene expression changes induced by AAV in both single and double doses revealed a lack of significant immune activation, as assessed by the lack of consistent expression of STAT1, a pro-inflammatory transcription factor, across groups (**Fig. 4E**).

We also analyzed the clonal expansion of B cells or T cells by measuring single-cell BCR and TCR clonal frequencies. Single and double AAV injections did not result in the clonal expansion of B cells or T cells (**Fig. 4F-G, Supplementary Fig. 5D-E**). However, we found that the number of clonotypes from both BCR and TCR in the single injection group increased compared to control and double injections. This result indicates an expansion of clonal diversity following the first but not second virus administration. Taken together, we have confirmed that the single administration of AAV can change a specific B cell subset compared to control buffer

injection. Interestingly, the lack of strong inflammatory or other immune cell expression changes suggests that mechanisms other than acute immune signaling, such as circulating antibodies, may play an important role in the neutralization of the AAV vector.

Elimination of IgG antibodies alone is not sufficient to enable AAV re-administration

To further explore the role of B cells in inhibiting AAV re-administration, we used an antibody cocktail to deplete B cells in C57BL/6 mice. Mice were given a second AAV administration of AAV-SEAP 3 weeks after the initial treatment and taken down another 3 weeks later. At the time of taking down, CD19+ B cells were completely depleted in the liver, spleen, and blood as measured by flow cytometry (**Fig. 5A**). CD4+ and CD8+ T cells were decreased but not completely depleted in the spleen (**Fig. 5B-C**). Viral DNA and transcripts from re-administration were not detected in the liver, and no protein product from re-administration was detected in the blood of depleted mice (**Fig. 5D**). Tracking the antibodies present in these animals showed that they had detectable NAb levels, unlike the μMT and R2G2 groups, but at significantly decreased levels compared to non-depleted WT mice (**Fig. 5E**). Further analysis of antibody isotype showed that anti-AAV9 IgGs were not detectable in depletion mice (**Fig. 5F**). However, anti-AAV9 IgM response was robust and persistent throughout the 6 weeks of the study. Taken together, these data suggest that our B-cell regimen was able to deplete CD19+ B cells such that anti-AAV9 IgG production was prevented, but anti-AAV9 IgM persisted, ultimately leading to the neutralization of AAV9.

AAV transduction efficiency of the brain is enhanced in μMT mice compared to wild-type mice

Lastly, AAV delivery to the brain through systemic administration is a major challenge due to the requirement to cross the blood-brain barrier, which results in low transduction efficiency and requires a large amount of AAVs. The ability to efficiently transduce the brain could be useful for fundamental neuroscience studies[60-62], and potentially in the treatment of genetic disorders of the CNS. Consequently, we investigated whether gene delivery to the brain can be enhanced in μMT mice compared to WT animals. PHP.eB AAV allows for efficient brain-wide transduction through systemic injection[63]. μMT and WT mice were injected with a single high dose (4.5e9 VP/g), single low dose (1.5e9 VP/g), or three weekly repeated low doses (1.5e9 VP/g) of PHP.eB packaged with GFP driven by CAG promoter (**Fig. 6A**). Three weeks after the last injections, the mice brains were extracted, sectioned, and imaged to quantify the GFP positive area of different brain regions, including striatum, cortex, hippocampus, and midbrain. In both μMT and WT mice, each region was transduced to an equal extent ($P > 0.9$), suggesting the average transduction efficiency is a reliable measure of the efficacy of transduction (**Fig. 6B-C**). We found that a single high dose of AAV resulted in a significantly increased positive pixel count for transduction in μMT mice compared to WT mice (15.6-fold higher, $P < 0.0002$, **Fig. 6D**). Interestingly, a single low dose for μMT was sufficient to reach similar GFP expression as the single high dose of WT mice, further suggesting enhancement of delivery in μMT mice ($P > 0.9$). Together, our results show μMT mice allow for improved delivery of AAVs to the brain, suggesting a critical role of B-cell mediated neutralization of AAVs even in cases of a single AAV administration.

Discussion

The host immune response against AAV vectors is a major hurdle for achieving efficacious and reliable gene therapy. We identified the absence of B cells as sufficient for allowing systemic AAV re-administration in mice. Furthermore, we showed that the presence of any anti-AAV IgM or IgG prevents AAV transduction in mice. Additionally, we showed that while various factors of the innate immune system may contribute to the anti-AAV immune response, elimination of these factors alone does not enable AAV re-administration.

This study provides systematic evidence that B cells are the key immune component in preventing AAV re-administration. Previous studies have described successful AAV re-administration in these mice. For example, Lorain *et al.* showed that multiple intramuscular administration was possible for AAV serotype 1 and, to a lesser degree, serotype 2 in μMT mice[64]. Siders *et al.* also showed that intravenous AAV2 administration was possible in μMT mice that have previously been immunized with AAV2 capsid protein[65]. Our results place the importance of the B cell in the context of other components of the innate and adaptive immune system. Using a panel of mice bred from a similar genetic background (C57BL/7 background), we can infer the relative importance of the various immune deficiencies available in the panel. Our panel included mice with deficiencies in macrophages, C3 complement, TLR9, MyD88, IL15 signaling, T cells, and B cells. We found only two mice strains in which systemic AAV re-administration was possible: the μMT and R2G2 mice. The R2G2 mouse is an ultra-immunodeficient animal model with knockout mutations in the *IL2RG* and *Rag2*, with deficiencies in T cells, B cells, NK cells, dendritic cells, macrophages, neutrophils, and receptors for a variety of cytokines[53]. The lack of B cells is the only overlapping deficiency in the two strains identified from our panel, suggesting that the lack of B cells is likely the primary factor for allowing AAV re-administration. The immune system is complex and involves numerous redundant pathways, and thus it is also likely that

secondary factors are involved in preventing AAV re-administration. However, if these secondary factors were present in our mouse panel, their effects alone were not significant enough to allow for AAV re-administration.

In combination with previous studies, our findings illustrate the complexity of the immune response to AAV and highlight the challenges in devising a therapeutic to allow re-administration. Nude mice lack functional T cells and therefore have deficiencies in immunoglobulin isotype switching. Thus, as expected and shown in previous studies[66,67], AAV administration in nude mice results in robust IgM formation with no detectable IgG formation (**Fig. 2**). A previous study with AAV serotype 2 found that tail-vein injection did not generate anti-AAV2 neutralizing antibodies and allowed for re-administration 28 days following initial injection[67]. However, in the current study, we found that injection of AAV serotype 9 resulted in neutralizing antibody generation, though at a level lower than in immunocompetent mice, and that AAV9 re-administration was not successful 21 days following initial injection (**Fig. 1** and **Fig. 2**). The immune response to AAV differs based on viral serotype[64,68], which may be the case for intravenously administered AAV2 and AAV9. Moreover, the difference in timing of re-administration (21 days in the current study vs. 28 days in[67]) may contribute to the differences in our findings.

Furthermore, our results show that eliminating components of the innate immune system does not allow for AAV re-administration. However, while we were unable to successfully re-administer AAV in our panel of innate deficient mice, deficiency in some innate immune systems may significantly reduce humoral response against AAV. The role of TLR9 in anti-capsid antibody response has been inconsistent[34-36,69], though there is growing evidence that MyD88 is more important for the anti-capsid immune response while TLR9 plays a greater role in anti-transgene response[34]. Our results support this hypothesis, as we did not see reduced anti-AAV capsid

antibodies in TLR9 deficient mice (**Fig. 2**). We found that mice with deficiencies in the C3 complement protein and MyD88 had significantly lower anti-AAV9 neutralizing and IgG antibody levels than immunocompetent mice (**Fig. 2**). Our data corroborate previous studies' findings using $C3^{-/-}$[37] and $MyD88^{-/-}$ mice[34,36]. More recently, Moghadam *et al.* showed that downregulation of the *Myd88* gene using a CRISPR-based transcriptional repressor can also decrease, but not completely eliminate, anti-AAV antibody formation[70]. Despite the reduction in anti-AAV antibodies, we found that a second AAV administration did not produce any transgene products in C3 and MyD88 knockout mice (**Fig. 1**). Furthermore, both these groups had high IgM levels but have barely detectable ($C3^{-/-}$ mice) or undetectable ($MyD88^{-/-}$ mice) IgG levels, even after a second AAV administration (**Fig. 2**), suggesting that there may be defects in isotype switching in these mice. Since IgM is typically associated with acute infection and is short-lived, it is possible that lengthening the time between vector treatments will increase efficacy from repeated administrations. The lack of antibody isotype class switching[35] and the inability to re-administer AAV in $MyD88^{-/-}$ mice has been noted previously[34] but are novel findings in $C3^{-/-}$ mice. However, the study from Moghadam *et al.* suggests that CRISPR-based *Myd88* repression can also allow for AAV9 administration after immunization with AAV1, though the relative efficacy of repeated administrations can be further quantified[70]. Thus, the role of the innate immune system in anti-AAV response remains an area of active study. Our findings suggest that while the innate immune system can contribute significantly to the humoral response against AAV, solely targeting single components of the innate immune system may not be enough to achieve vector re-administration.

Analysis of the serum anti-AAV antibodies levels and their correlation with transgene production shows that neutralizing antibodies must be below the threshold of detection for AAV re-administration to be successful in mice (**Fig. 1** and **Fig. 2**). In the current study, the detection

limit for the *in vitro* NAb assay was 1:100, as the presence of greater amounts of serum led to changes in cell growth patterns that affected the neutralization curve. Our finding is in line with previous studies, in which neutralizing antibody titers greater than 1:5 were able to neutralize virus activity in non-human primates[59]. This result also suggests that IgM antibodies may play an important role in neutralizing AAV activity, as multiple immune-deficient mice strains ($C3^{-/-}$, $MyD88^{-/-}$, and nude mice) had persistent neutralizing IgM antibodies that contributed to detectable NAb titers (**Fig. 2**). Significantly, transient B cell depletion in C57BL/6 mice using an antibody cocktail was successful in eliminating IgG but not IgM production, ultimately resulting in AAV neutralization upon re-administration (**Fig. 5**). Taken together, our results support an antibody or B cell-focused approach, such as the use of immunoglobulin-cleaving enzymes[71], to eliminate the anti-AAV capsid immune response. These data also highlight the importance of complete elimination of anti-AAV capsid neutralizing antibodies for repeated AAV administrations. We further validated the use of μMT mice in AAV re-administration studies.

Multiple low doses of an AAV encoding GFP achieved similar GFP expression levels as a single equivalent large dose of AAV **(Fig. 6)**. In pre-clinical studies, μMT mice are a model that can be used to study repeated AAV dosing in a system with some functional immune compartments. Importantly, in this study, we found that PHP.eB AAV transduction of the brain was increased in the μMT mice **(Fig. 6)**. This improved transduction highlights the utility of μMT mice as a useful tool for neuroscience and neuro-engineering research. In homozygous μMT animals, B cell development is arrested at the stage of pre-B-cell maturation, and this pathway provides an important avenue for attenuation using targeted immunotherapy regimens to enable re-administration of AAV vectors[52].

In summary, we evaluated AAV re-administration in a panel of immune-deficient mice and found the absence of B cells to be sufficient for repeated intravenous administration of AAV9. We also found that both IgM and IgG antibodies contribute to the neutralization of AAV capsids. Successful vector re-administration requires the neutralizing antibody titer at the time of injection to be below *in vitro* assay level of detection. We confirmed previous studies that demonstrated that the innate immune system could profoundly affect the humoral response and found that deficiencies in individual components of the immune system were not enough to allow for repeated AAV administrations. Overall, our findings contribute to the study of the immune response against AAV and help inform the development of new strategies for evading the host immune response for improved AAV gene therapy.

References

1 Smalley, E. First AAV gene therapy poised for landmark approval. *Nature Biotechnology* **35**, 998-999, doi:10.1038/nbt1117-998 (2017).

2 Li, C. & Samulski, R. J. Engineering adeno-associated virus vectors for gene therapy. *Nature Reviews Genetics* **21**, 255-272, doi:10.1038/s41576-019-0205-4 (2020).

3 Manno, C. S. *et al.* Successful transduction of liver in hemophilia by AAV-Factor IX and limitations imposed by the host immune response. *Nat Med* **12**, 342-347, doi:10.1038/nm1358 (2006).

4 Boutin, S. *et al.* Prevalence of serum IgG and neutralizing factors against adeno-associated virus (AAV) types 1, 2, 5, 6, 8, and 9 in the healthy population: implications for gene therapy using AAV vectors. *Human gene therapy* **21**, 704-712 (2010).

5 Calcedo, R., Vandenberghe, Luk H., Gao, G., Lin, J. & Wilson, James M. Worldwide epidemiology of neutralizing antibodies to adeno-associated viruses. *The Journal of Infectious Diseases* **199**, 381-390, doi:10.1086/595830 (2009).

6 Calcedo, R. *et al.* Adeno-associated virus antibody profiles in newborns, children, and adolescents. *Clin. Vaccine Immunol.* **18**, 1586-1588, doi:10.1128/CVI.05107-11 (2011).

7 Erles, K., Sebökovà, P. & Schlehofer, J. R. Update on the prevalence of serum antibodies (IgG and IgM) to adeno-associated virus (AAV). *Journal of Medical Virology* **59**, 406-411, doi:10.1002/(SICI)1096-9071(199911)59:3<406::AID-JMV22>3.0.CO;2-N (1999).

8 Kruzik, A. *et al.* Prevalence of anti-adeno-associated virus immune responses in international cohorts of healthy donors. *Molecular Therapy - Methods & Clinical Development*, S2329050119300580, doi:10.1016/j.omtm.2019.05.014 (2019).

9 Leborgne, C. *et al.* Prevalence and long-term monitoring of humoral immunity against adeno-associated virus in Duchenne Muscular Dystrophy patients. *Cell. Immunol.*, doi:10.1016/j.cellimm.2018.03.004 (2018).

10 Liu, Q. *et al.* Neutralizing antibodies against AAV2, AAV5 and AAV8 in healthy and HIV-1-infected subjects in China: implications for gene therapy using AAV vectors. *Gene Therapy* **21**, 732-738, doi:10.1038/gt.2014.47 (2014).

11 George, L. A. *et al.* Hemophilia B gene therapy with a high-specific-activity factor IX variant. *New England Journal of Medicine* **377**, 2215-2227, doi:10.1056/NEJMoa1708538 (2017).

12 Rabinowitz, J., Chan, Y. K. & Richard Jude, S. Adeno-associated virus (AAV) versus immune response. *Viruses* **11**, doi:10.3390/v11020102 (2019).

13 Tse, L. V. *et al.* Structure-guided evolution of antigenically distinct adeno-associated virus variants for immune evasion. *Proceedings of the National Academy of Sciences* **114**, E4812-E4821, doi:10.1073/pnas.1704766114 (2017).

14 George, L. A. *et al.* Long-term follow-up of the first in human intravascular delivery of AAV for gene transfer: AAV2-hFIX16 for severe hemophilia B. *Molecular Therapy* **28**, 2073-2082, doi:10.1016/j.ymthe.2020.06.001 (2020).

15 Nathwani, A. C. *et al.* Long-term safety and efficacy of factor IX gene therapy in hemophilia B. *N Engl J Med* **371**, 1994-2004, doi:10.1056/NEJMoa1407309 (2014).

16 Rangarajan, S. *et al.* AAV5–Factor VIII gene transfer in severe hemophilia A. *New England Journal of Medicine* **377**, 2519-2530, doi:10.1056/NEJMoa1708483 (2017).

17 Weber, T. Anti-AAV Antibodies in AAV Gene Therapy: Current Challenges and Possible Solutions. *Front. Immunol.* **12**, doi:10.3389/fimmu.2021.658399 (2021).

18 Meliani, A. *et al.* Antigen-selective modulation of AAV immunogenicity with tolerogenic rapamycin nanoparticles enables successful vector re-administration. *Nature Communications* **9**, 4098, doi:10.1038/s41467-018-06621-3 (2018).

19 Calcedo, R. & Wilson, J. Humoral Immune Response to AAV. *Front. Immunol.* **4**, doi:10.3389/fimmu.2013.00341 (2013).

20 Duan, D. *et al.* Circular Intermediates of Recombinant Adeno-Associated Virus Have Defined Structural Characteristics Responsible for Long-Term Episomal Persistence in Muscle Tissue. *Journal of Virology* **72**, 8568-8577 (1998).

21 Schnepp, B. C., Clark, K. R., Klemanski, D. L., Pacak, C. A. & Johnson, P. R. Genetic fate of recombinant adeno-associated virus vector genomes in muscle. *Journal of Virology* **77**, 3495-3504, doi:10.1128/JVI.77.6.3495-3504.2003 (2003).

22 Schnepp, B. C., Jensen, R. L., Chen, C.-L., Johnson, P. R. & Clark, K. R. Characterization of adeno-associated virus genomes isolated from human tissues. *Journal of Virology* **79**, 14793-14803, doi:10.1128/JVI.79.23.14793-14803.2005 (2005).

23 Naso, M. F., Tomkowicz, B., Perry, W. L. & Strohl, W. R. Adeno-associated virus (AAV) as a vector for gene therapy. *BioDrugs* **31**, 317-334, doi:10.1007/s40259-017-0234-5 (2017).

24 Wang, L., Wang, H., Bell, P., McMenamin, D. & Wilson, J. M. Hepatic gene transfer in neonatal mice by adeno-associated virus serotype 8 vector. *Human Gene Therapy* **23**, 533-539, doi:10.1089/hum.2011.183 (2012).

25 Pasi, K. J. *et al.* Multiyear Follow-up of AAV5-hFVIII-SQ Gene Therapy for Hemophilia A. *New England Journal of Medicine* **382**, 29-40, doi:10.1056/NEJMoa1908490 (2020).

26 Colella, P., Ronzitti, G. & Mingozzi, F. Emerging Issues in AAV-Mediated In Vivo Gene Therapy. *Molecular Therapy - Methods & Clinical Development* **8**, 87-104, doi:10.1016/j.omtm.2017.11.007 (2018).

27 Muhuri, M. *et al.* Overcoming innate immune barriers that impede AAV gene therapy vectors. *J Clin Invest* **131**, doi:10.1172/JCI143780 (2021).

28 Eixarch, H. *et al.* Transgene Expression Levels Determine the Immunogenicity of Transduced Hematopoietic Grafts in Partially Myeloablated Mice. *Molecular Therapy* **17**, 1904-1909, doi:10.1038/mt.2009.198 (2009).

29 Sargent, D. *et al.* Investigating the neuroprotective effect of AAV-mediated β-synuclein overexpression in a transgenic model of synucleinopathy. *Scientific Reports* **8**, 17563, doi:10.1038/s41598-018-35825-2 (2018).

30 Ronzitti, G., Gross, D.-A. & Mingozzi, F. Human immune responses to adeno-associated virus (AAV) vectors. *Front. Immunol.* **11**, 670, doi:10.3389/fimmu.2020.00670 (2020).

31 Zaiss, A. K. *et al.* Differential activation of innate immune responses by adenovirus and adeno-associated virus vectors. *Journal of Virology* **76**, 4580-4590, doi:10.1128/JVI.76.9.4580-4590.2002 (2002).

32 Verdera, H. C., Kuranda, K. & Mingozzi, F. AAV vector immunogenicity in humans: a long journey to successful gene transfer. *Molecular Therapy* **28**, 723-746, doi:10.1016/j.ymthe.2019.12.010 (2020).

33 Ashley, S. N., Somanathan, S., Giles, A. R. & Wilson, J. M. TLR9 signaling mediates adaptive immunity following systemic AAV gene therapy. *Cell. Immunol.* **346**, 103997, doi:10.1016/j.cellimm.2019.103997 (2019).

34 Rogers, G. L. *et al.* Unique roles of TLR9- and MyD88-dependent and -independent pathways in adaptive immune responses to AAV-mediated gene transfer. *J Innate Immun* **7**, 302-314, doi:10.1159/000369273 (2015).

35 Sudres, M. *et al.* MyD88 signaling in B cells regulates the production of Th1-dependent antibodies to AAV. *Molecular Therapy* **20**, 1571-1581, doi:10.1038/mt.2012.101 (2012).

36 Zhu, J., Huang, X. & Yang, Y. The TLR9-MyD88 pathway is critical for adaptive immune responses to adeno-associated virus gene therapy vectors in mice. *J Clin Invest* **119**, 2388-2398, doi:10.1172/JCI37607 (2009).

37 Zaiss, A. K. *et al.* Complement is an essential component of the immune response to adeno-associated virus vectors. *Journal of Virology* **82**, 2727-2740, doi:10.1128/JVI.01990-07 (2008).

38 Hui, D. J. *et al.* AAV capsid CD8+ T-cell epitopes are highly conserved across AAV serotypes. *Molecular Therapy - Methods & Clinical Development* **2**, 15029, doi:10.1038/mtm.2015.29 (2015).

39 Mingozzi, F. *et al.* CD8+ T-cell responses to adeno-associated virus capsid in humans. *Nat Med* **13**, 419-422, doi:10.1038/nm1549 (2007).

40 Pien, G. C. *et al.* Capsid antigen presentation flags human hepatocytes for destruction after transduction by adeno-associated viral vectors. *J Clin Invest* **119**, 1688-1695, doi:10.1172/JCI36891 (2009).

41 Shirley, J. L. *et al.* Type I IFN sensing by cDCs and CD4+ T cell help are both requisite for cross-priming of AAV capsid-specific CD8+ T cells. *Molecular Therapy* **28**, 758-770, doi:10.1016/j.ymthe.2019.11.011 (2020).

42 Bočkor, L. *et al.* Repeated AAV-mediated gene transfer by serotype switching enables long-lasting therapeutic levels of hUgt1a1 enzyme in a mouse model of Crigler–Najjar Syndrome Type I. *Gene Therapy* **24**, 649-660, doi:10.1038/gt.2017.75 (2017).

43 Majowicz, A. *et al.* Successful repeated hepatic gene delivery in mice and non-human primates achieved by sequential administration of AAV5ch and AAV1. *Molecular Therapy* **25**, 1831-1842, doi:10.1016/j.ymthe.2017.05.003 (2017).

44 Ge, Y., Powell, S., Roey, M. V. & McArthur, J. G. Factors influencing the development of an anti–factor IX (FIX) immune response following administration of adeno-associated virus–FIX. *Blood* **97**, 3733-3737, doi:10.1182/blood.V97.12.3733 (2001).

45 McIntosh, J. H. *et al.* Successful attenuation of humoral immunity to viral capsid and transgenic protein following AAV-mediated gene transfer with a non-depleting CD4 antibody and cyclosporine. *Gene Therapy* **19**, 78-85, doi:10.1038/gt.2011.64 (2012).

46 Mingozzi, F. *et al.* Pharmacological modulation of humoral immunity in a nonhuman primate model of AAV gene transfer for hemophilia B. *Molecular Therapy* **20**, 1410-1416, doi:10.1038/mt.2012.84 (2012).

47 Monteilhet, V. *et al.* A 10 patient case report on the impact of plasmapheresis upon neutralizing factors against adeno-associated virus (AAV) types 1, 2, 6, and 8. *Molecular Therapy* **19**, 2084-2091, doi:10.1038/mt.2011.108 (2011).

48 Orlowski, A. *et al.* Successful transduction with AAV vectors after selective depletion of anti-AAV antibodies by immunoadsorption. *Molecular Therapy - Methods & Clinical Development* **16**, 192-203, doi:10.1016/j.omtm.2020.01.004 (2020).

49 Corti, M. *et al.* B-cell depletion is protective against anti-AAV capsid immune response: a human subject case study. *Molecular Therapy - Methods & Clinical Development* **1**, 14033, doi:10.1038/mtm.2014.33 (2014).

50 Goldszmid, Romina S., Dzutsev, A. & Trinchieri, G. Host Immune Response to Infection and Cancer: Unexpected Commonalities. *Cell Host & Microbe* **15**, 295-305, doi:10.1016/j.chom.2014.02.003 (2014).

51 Kitamura, D., Roes, J., Kühn, R. & Rajewsky, K. A B cell-deficient mouse by targeted disruption of the membrane exon of the immunoglobulin f.l chain gene. **350**, 4, doi:10.1038/350423a0 (1991).

52 Lee, D. S. W., Rojas, O. L. & Gommerman, J. L. B cell depletion therapies in autoimmune disease: advances and mechanistic insights. *Nature Reviews Drug Discovery* **20**, 179-199, doi:10.1038/s41573-020-00092-2 (2021).

53 Envigo. Rag2-Il2rg double knockout mice (R2G2®) B6;129-Rag2tm1FwaIl2rgtm1Rsky/DwlHsd. *Envigo* (2020).

54 Ho, M. L., Adler, B. A., Torre, M. L., Silberg, J. J. & Suh, J. SCHEMA computational design of virus capsid chimeras: calibrating how genome packaging, protection, and transduction correlate with calculated structural disruption. *ACS Synthetic Biology* **2**, 724-733, doi:10.1021/sb400076r (2013).

55 Penaranda, C., Tang, Q. & Bluestone, J. A. Anti-CD3 therapy promotes tolerance by selectively depleting pathogenic cells while preserving regulatory T cells. *J Immunol* **187**, 2015-2022, doi:10.4049/jimmunol.1100713 (2011).

56 Schuster, D. J. *et al.* Biodistribution of adeno-associated virus serotype 9 (AAV9) vector after intrathecal and intravenous delivery in mouse. *Front Neuroanat* **8**, doi:10.3389/fnana.2014.00042 (2014).

57 Srivastava, A. In vivo tissue-tropism of adeno-associated viral vectors. *Current Opinion in Virology* **21**, 75-80, doi:10.1016/j.coviro.2016.08.003 (2016).

58 Zincarelli, C., Soltys, S., Rengo, G. & Rabinowitz, J. E. Analysis of AAV serotypes 1–9 mediated gene expression and tropism in mice after systemic injection. *Molecular Therapy* **16**, 1073-1080, doi:10.1038/mt.2008.76 (2008).

59 Wang, L. *et al.* Impact of pre-existing immunity on gene transfer to nonhuman primate liver with adeno-associated virus 8 vectors. *Human Gene Therapy* **22**, 1389-1401, doi:10.1089/hum.2011.031 (2011).

60 Peters, C. W., Maguire, C. A. & Hanlon, K. S. Delivering AAV to the Central Nervous and Sensory Systems. *Trends in Pharmacological Sciences* **42**, 461-474, doi:10.1016/j.tips.2021.03.004 (2021).

61 Haggerty, D. L., Grecco, G. G., Reeves, K. C. & Atwood, B. Adeno-Associated Viral Vectors in Neuroscience Research. *Molecular Therapy - Methods & Clinical Development* **17**, 69-82, doi:10.1016/j.omtm.2019.11.012 (2020).

62 Galvan, A. *et al.* Nonhuman Primate Optogenetics: Recent Advances and Future Directions. *The Journal of Neuroscience* **37**, 10894, doi:10.1523/JNEUROSCI.1839-17.2017 (2017).

63 Chan, K. Y. *et al.* Engineered AAVs for efficient noninvasive gene delivery to the central and peripheral nervous systems. *Nature Neuroscience* **20**, 1172-1179, doi:10.1038/nn.4593 (2017).

64 Lorain, S. *et al.* Transient immunomodulation allows repeated injections of AAV1 and correction of muscular dystrophy in multiple muscles. *Molecular Therapy* **16**, 541-547, doi:10.1038/sj.mt.6300377 (2008).

65 Siders, W. M. *et al.* Cytotoxic T lymphocyte responses to transgene product, not adeno-associated viral capsid protein, limit transgene expression in mice. *Human Gene Therapy* **20**, 11-20, doi:10.1089/hum.2008.055 (2009).

66 Chirmule, N. *et al.* Humoral immunity to adeno-associated virus type 2 vectors following administration to murine and nonhuman primate muscle. *Journal of Virology* **74**, 2420-2425, doi:10.1128/JVI.74.5.2420-2425.2000 (2000).

67 Xiao, W. *et al.* Route of administration determines induction of T-cell-independent humoral responses to adeno-associated virus vectors. *Molecular Therapy* **1**, 323-329, doi:10.1006/mthe.2000.0045 (2000).

68 Xin, K.-Q. *et al.* Induction of robust immune responses against human immunodeficiency virus is supported by the inherent tropism of adeno-associated virus type 5 for dendritic cells. *Journal of Virology* **80**, 11899-11910, doi:10.1128/JVI.00890-06 (2006).

69 Martino, A. T. *et al.* The genome of self-complementary adeno-associated viral vectors increases Toll-like receptor 9–dependent innate immune responses in the liver. *Blood* **117**, 6459-6468, doi:10.1182/blood-2010-10-314518 (2011).

70 Moghadam, F. *et al.* Synthetic immunomodulation with a CRISPR super-repressor in vivo. *Nature Cell Biology* **22**, 1143-1154, doi:10.1038/s41556-020-0563-3 (2020).

71 Leborgne, C. *et al.* IgG-cleaving endopeptidase enables in vivo gene therapy in the presence of anti-AAV neutralizing antibodies. *Nat Med*, 1-6, doi:10.1038/s41591-020-0911-7 (2020).

Acknowledgements

This work was supported by the National Institutes of Health under grant numbers grant numbers R01CA207497 to J.S., NIH fellowship (F30HL146032) to M.C. This work was supported by Cancer Prevention Research Institute of Texas grant RR160047 to O.V., and Rice University Academy Fellowship to M.I.J. The authors acknowledge the use of equipment at the Shared Equipment Authority of Rice University. The authors would also like to acknowledge the support of the Single Cell Genomics Core at Baylor College of Medicine, partially supported by NIH shared instrument grants (S10OD023469, S10OD025240) and P30EY002520.

Author Contributions

Conceptualization: M.C., B.K., M.I.J., J.S., O.V. Methodology: M.C., B.K., M.I.J., S.F., S.D., S.N., S.B., S.L., C.C., H.C.H., J.O.S., J.S., O.V. Investigation: M.C., B.K., M.I.J., S.F., S.D., S.N., S.B., S.L., C.C. Visualization: M.C., B.K., M.I.J., S.F., S.N., S.L., C.C. Supervision:

H.C.H., J.O.S., J.S., O.V. Writing: M.C., B.K., M.I.J., S.F., S.N., S.L., C.C., H.C.H., J.O.S., J.S., O.V.

Competing Interests

J.S. is an employee of Biogen Inc. as of 2019. O.V. is a member of the Scientific Advisory Board of Sigilon Therapeutics and holds equity in the Avenge Bio and Pana Bio.

Figure legends

Fig 1. Re-administration of AAV in the panel of immune-deficient mice. **A**, Simplified schematic of innate and adaptive immune response to AAV administration. (1) Antigen-presenting cells (APCs) of the innate immune system can take up AAV in a process mediated by complement proteins (2). Once inside the APC, the viral genome is recognized by Toll-like receptor 9 (TLR9) (3), resulting in the activation of various signaling pathways, including those mediated by adaptor molecule MyD88 (4), ultimately resulting in APC activation and production of inflammatory cytokines that activate the adaptive immune system. Within the adaptive immune system, the activation of B cells (5), aided by CD4+ T cells (6), leads to the humoral response, which involves the production of antibodies capable of neutralizing AAV. CD8+ T cell (7) activation is the basis for cell-based immunity, resulting in the destruction of transduced cells. **B**, Summary of mouse strains used in this study, with numbers corresponding to those labeled in part **A**. **C**, Timeline of AAV re-administration studies. MLuc and SEAP correspond to single-injection controls, and double corresponds to double injection in WT mice. All innate (blue) and adaptive (orange) panels were received double injections (1st MLuc and 2nd SEAP injections). **D**, Viral DNA and **E**, transgene mRNA were extracted from mouse livers 6 weeks after initial AAV injection. mRNA was reverse-transcribed. Both were quantified for MLuc and SEAP levels with qPCR. **F**, SEAP level in the serum at week 6 was assayed and normalized to the level of expression from single AAV9-SEAP expression in WT mice. N = 4-8 animals per group. * indicates $P < 0.05$ compared to single injection in WT mice, as measured by 1-way ANOVA with Tukey post-hoc testing.

Fig 2. Neutralizing, IgM, and IgG antibody profiles after single and double injection. **A**, Neutralizing antibody (NAb) titers were measured using an *in vitro* assay for AAV9-MLuc single injection (MLuc), AAV9-SEAP single injection (SEAP), or double injection (Double) groups. Titers are plotted as reciprocal of the dilution necessary to neutralize 50% of virus activity. **B**, NAb titers for single and double injection control groups and for immune-deficient mice group panel. *

indicates $P < 0.05$ when compared with the value from week 3, and + indicates $P < 0.05$ when compared with the value from week 4, as measured by two-way ANOVA with Tukey post-hoc testing. **C**, IgM and IgG in mice after single injection of AAV9-MLuc. **D**, IgM and IgG in double injection mice as measured by ELISA. **E**, IgM and **F**, IgG levels in immune-deficient mice, with * indicating $P < 0.05$ compared to the prior time point shown, as measured by 2-way ANOVA with Tukey post-hoc testing. N = 4-8 animals per group.

Fig 3. Biodistribution of single and double AAV administrations in WT mice. A, Viral genomes and **B**, mRNA transcripts were measured after a single injection of AAV9-MLuc or AAV-SEAP in separate mice groups. Two-way ANOVA was performed and did not indicate significance between MLuc and SEAP measurements. **C**, Viral genomes, and **D**, mRNA transcripts were measured after two AAV administrations in the same animal: AAV9-MLuc at week 0 and AAV9-SEAP at week 3. Mice were taken down for processing at week 6. * indicates $P < 0.05$ as measured by 2-way ANOVA with Sidak post-hoc testing. Dotted line indicates the threshold of detection based on the lowest standard for qPCR-based assays. Values below the threshold were not considered for statistical analysis. N=4-5 mice per group.

Fig 4. Re-administration of AAV does not alter splenic immune composition. A, tSNE embedding of individual cells pooled from all three samples (control, single administration AAV, double administration AAV). The resulting clusters are classified by immune cell type based on cell-specific expression profiles (shown in **Supplementary Fig. 5B**). **B**, Immune composition of the spleen 1 week after final AAV administration. **C**, Graph-based clustering of B cell subsets across all 3 conditions. **D**, Relative abundance of each B cell cluster in each condition. **E**, Expression of STAT1 across conditions. **F**, Relative abundance of the top 10 most abundant BCR clonotypes for each condition. **G**, Relative abundance of the top 10 most abundant TCR clonotypes for each condition.

Fig 5. Antibody cocktail depletion of B- and T-Cells in C57BL/6 mice. Flow cytometry was used to quantify **A**, CD19+, **B**, CD4+, and **C**, CD8+ cells in spleen, liver, and blood of depletion mice 7 weeks after initiating weekly antibody cocktail IP administration. * indicates $P < 0.05$ as measured by 2-way ANOVA with Tukey post-hoc testing. **D**, Viral DNA and mRNA from the second AAV administration, AAV-SEAP, was measured in the liver using qPCR or RT-qPCR. SEAP protein expression was quantified in the serum three weeks after re-administration. Values were normalized by levels in singly injected mice. **E**, Neutralizing antibody titer of double injection in WT (Double), depletion group, μMT, and R2G2 mice over the course of the study as measured by *in vitro* NAb assay. **F**, IgM and IgG in depletion mice over 6 weeks, as measured by ELISAs. n = 4 animals per group.

Fig 6. Re-administration of CAG-NLS-GFP PHP.eB to the brain. A, Timeline of re-administration studies (n=5 animals per group). μMT and WT mice were injected with a single high dose (4.5e9 VP/g), single low dose (1.5e9 VP/g), or three weekly repeated low doses (1.5e9

VP/g) of PHP.eB packaged with GFP driven by CAG promoter. **B**, Representative images of GFP expression in each brain region. **C**, Quantification of GFP expression by brain region defined as area above a threshold of 15 in ImageJ (N=5 animals per group). ns (not significant) not shown between regions in the same dose group, using 3-way ANOVA Tukey's testing. **D**, Average area GFP expression in the brain regions measured in **C**. *** indicates $P < 0.0002$ compared to other groups as measured by 2-way ANOVA with Tukey's post-hoc testing.

Figures

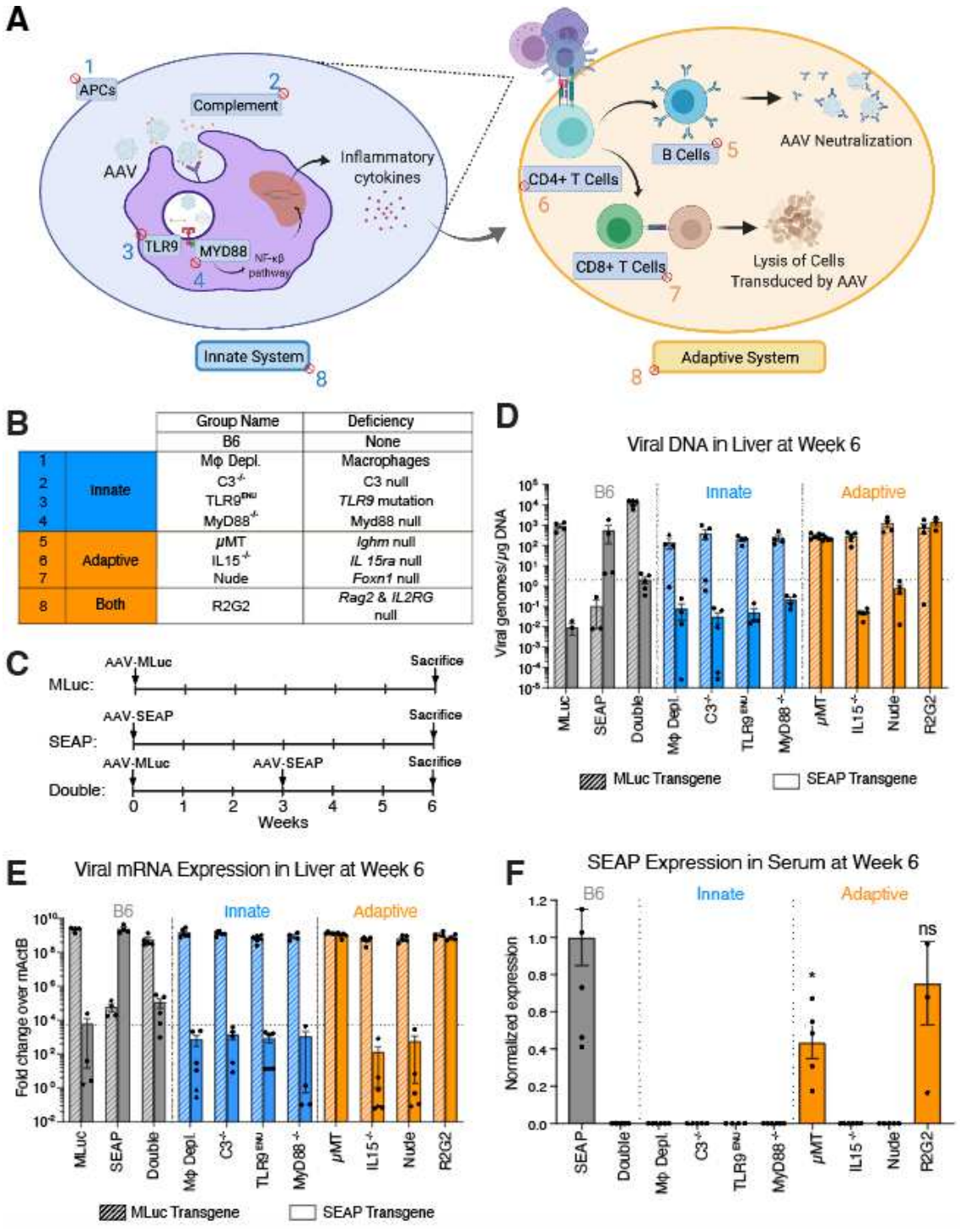

Fig 1. Re-administration of AAV in the panel of immune-deficient mice. **A**, Simplified schematic of innate and adaptive immune response to AAV administration. (1) Antigen-presenting cells (APCs) of the innate immune system can take up AAV in a process mediated by complement proteins (2). Once inside

the APC, the viral genome is recognized by Toll-like receptor 9 (TLR9) (3), resulting in the activation of various signaling pathways, including those mediated by adaptor molecule MyD88 (4), ultimately resulting in APC activation and production of inflammatory cytokines that activate the adaptive immune system. Within the adaptive immune system, the activation of B cells (5), aided by CD4+ T cells (6), leads to the humoral response, which involves the production of antibodies capable of neutralizing AAV. CD8+ T cell (7) activation is the basis for cell-based immunity, resulting in the destruction of transduced cells. **B**, Summary of mouse strains used in this study, with numbers corresponding to those labeled in part **A**. **C**, Timeline of AAV re-administration studies. MLuc and SEAP correspond to single-injection controls, and double corresponds to double injection in WT mice. All innate (blue) and adaptive (orange) panels were received double injections (1st MLuc and 2nd SEAP injections). **D**, Viral DNA and **E**, transgene mRNA were extracted from mouse livers 6 weeks after initial AAV injection. mRNA was reverse-transcribed. Both were quantified for MLuc and SEAP levels with qPCR. **F**, SEAP level in the serum at week 6 was assayed and normalized to the level of expression from single AAV9-SEAP expression in WT mice. N = 4-8 animals per group. * indicates $P < 0.05$ compared to single injection in WT mice, as measured by 1-way ANOVA with Tukey post-hoc testing.

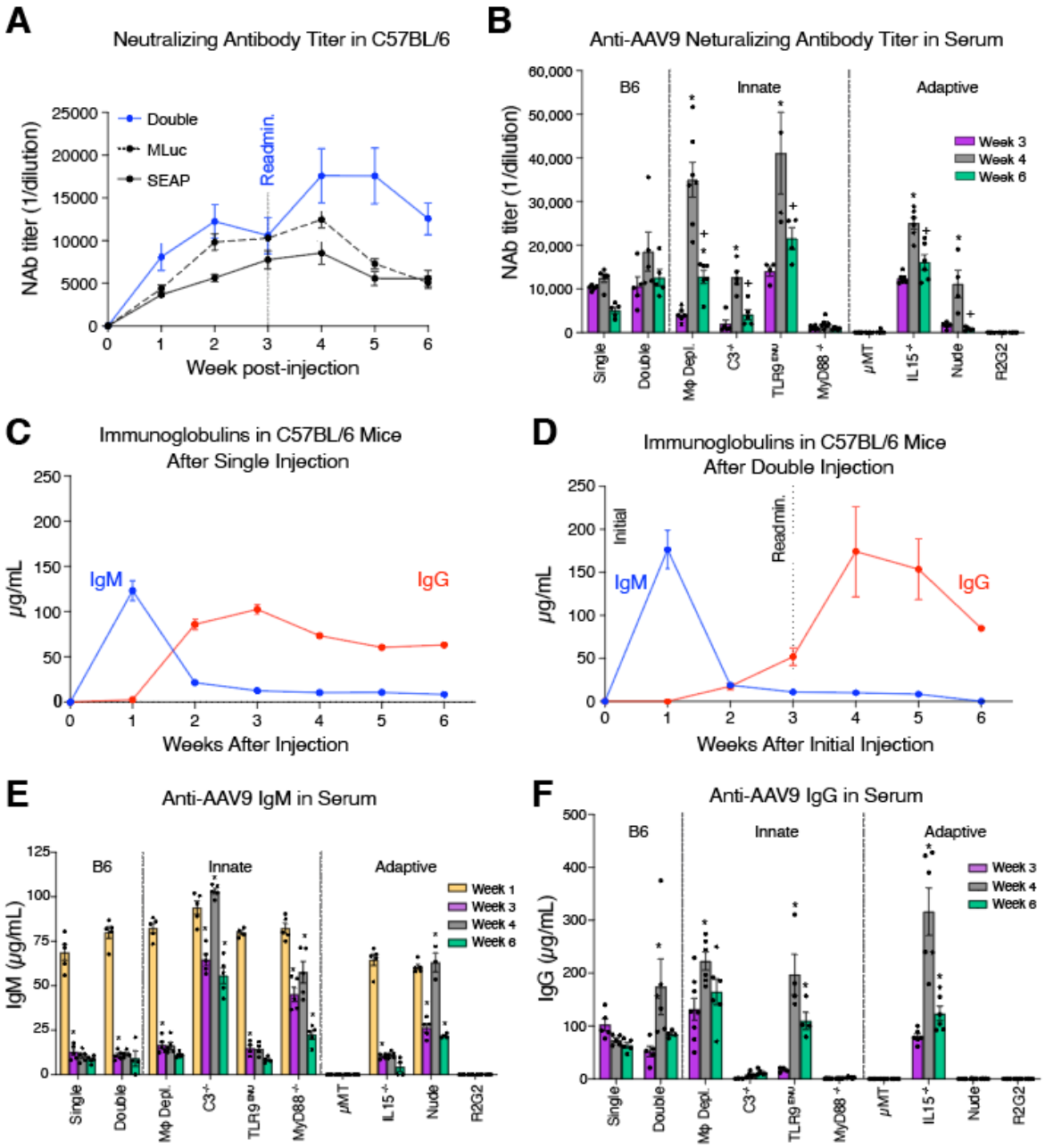

Fig 2. Neutralizing, IgM, and IgG antibody profiles after single and double injection. **A**, Neutralizing antibody (NAb) titers were measured using an *in vitro* assay for AAV9-MLuc single injection (MLuc), AAV9-SEAP single injection (SEAP), or double injection (Double) groups. Titers are plotted as reciprocal of the dilution necessary to neutralize 50% of virus activity. **B**, NAb titers for single and double injection control groups and for immune-deficient mice group panel. * indicates $P < 0.05$ when compared with the value from week 3, and + indicates $P < 0.05$ when compared with the value from week 4, as measured by two-way ANOVA with Tukey post-hoc testing. **C**, IgM and IgG in mice after single injection of AAV9-MLuc. **D**, IgM and IgG in double injection mice as measured by ELISA. **E**, IgM and **F**, IgG levels in immune-deficient mice, with * indicating $P < 0.05$ compared to the prior time point shown, as measured by 2-way ANOVA with Tukey post-hoc testing. N = 4-8 animals per group.

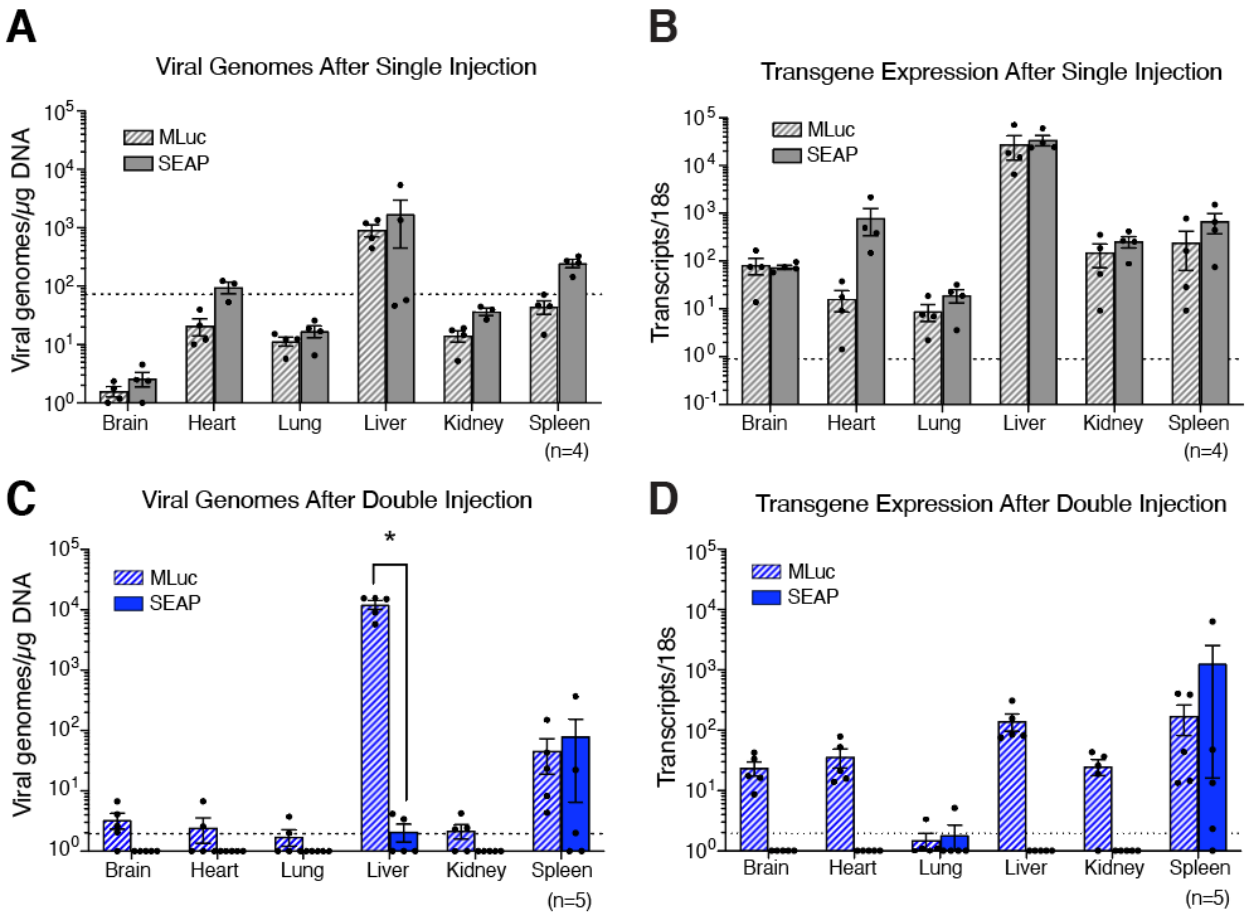

Fig 3. Biodistribution of single and double AAV administrations in WT mice. A, Viral genomes and **B**, mRNA transcripts were measured after a single injection of AAV9-MLuc or AAV-SEAP in separate mice groups. Two-way ANOVA was performed and did not indicate significance between MLuc and SEAP measurements. **C**, Viral genomes, and **D**, mRNA transcripts were measured after two AAV administrations in the same animal: AAV9-MLuc at week 0 and AAV9-SEAP at week 3. Mice were taken down for processing at week 6. * indicates $P < 0.05$ as measured by 2-way ANOVA with Sidak post-hoc testing. Dotted line indicates the threshold of detection based on the lowest standard for qPCR-based assays. Values below the threshold were not considered for statistical analysis. N=4-5 mice per group.

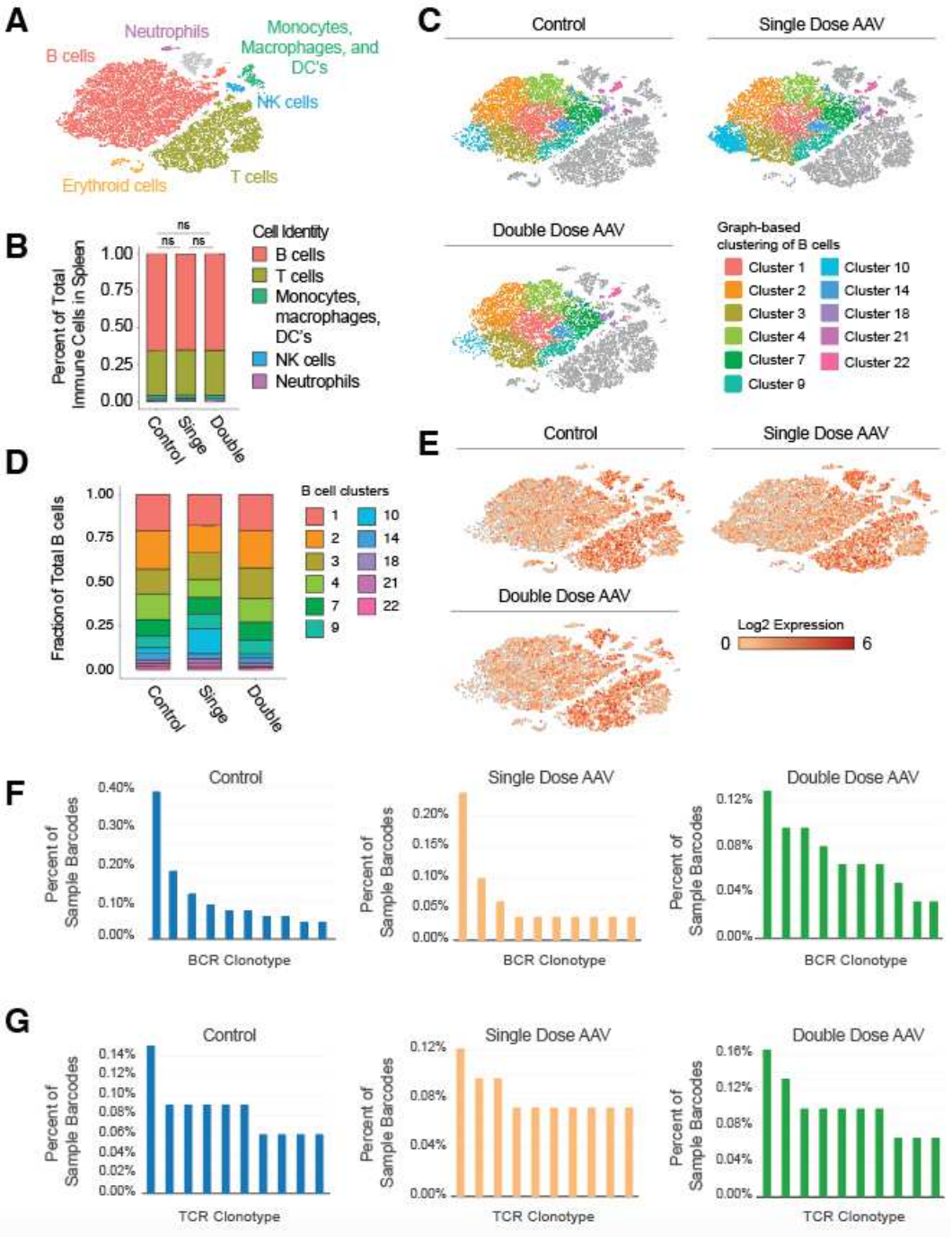

Fig 4. Re-administration of AAV does not alter splenic immune composition. A, tSNE embedding of individual cells pooled from all three samples (control, single administration AAV, double administration AAV). The resulting clusters are classified by immune cell type based on cell-specific expression profiles (shown in **Supplementary Fig. 5B**). **B**, Immune composition of the spleen 1 week after final AAV administration. **C**, Graph-based clustering of B cell subsets across all 3 conditions. **D**, Relative abundance of each B cell cluster in each condition. **E**, Expression of STAT1 across conditions. **F**, Relative abundance of the top 10 most abundant BCR clonotypes for each condition. **G**, Relative abundance of the top 10 most abundant TCR clonotypes for each condition.

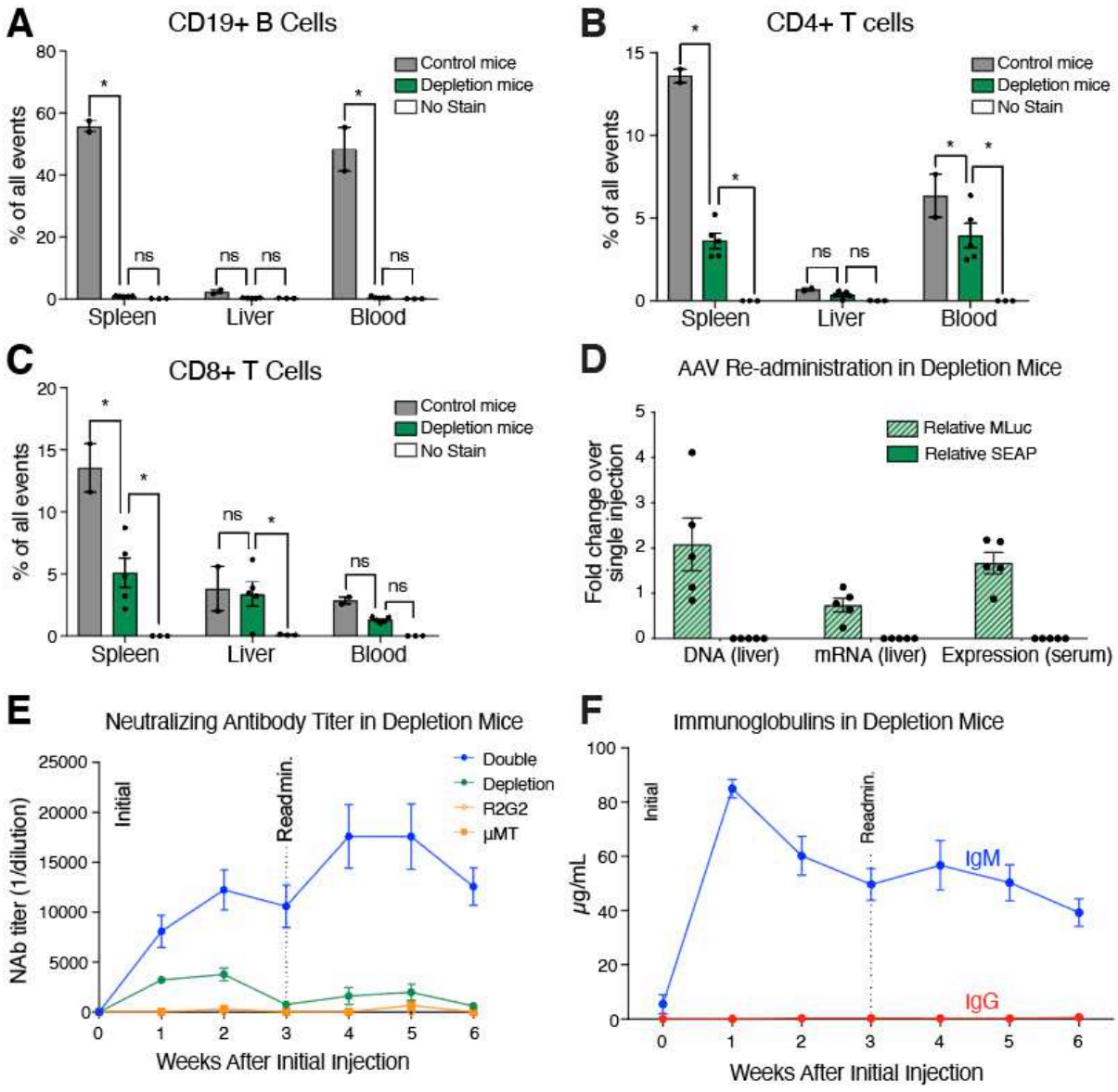

Fig 5. Antibody cocktail depletion of B- and T-Cells in C57BL/6 mice. Flow cytometry was used to quantify **A**, CD19+, **B**, CD4+, and **C**, CD8+ cells in spleen, liver, and blood of depletion mice 7 weeks after initiating weekly antibody cocktail IP administration. * indicates $P < 0.05$ as measured by 2-way ANOVA with Tukey post-hoc testing. **D**, Viral DNA and mRNA from the second AAV administration, AAV-SEAP, was measured in the liver using qPCR or RT-qPCR. SEAP protein expression was quantified in the serum three weeks after re-administration. Values were normalized by levels in singly injected mice. **E**, Neutralizing antibody titer of double injection in WT (Double), depletion group, µMT, and R2G2 mice over the course of the study as measured by *in vitro* NAb assay. **F**, IgM and IgG in depletion mice over 6 weeks, as measured by ELISAs. n = 4 animals per group.

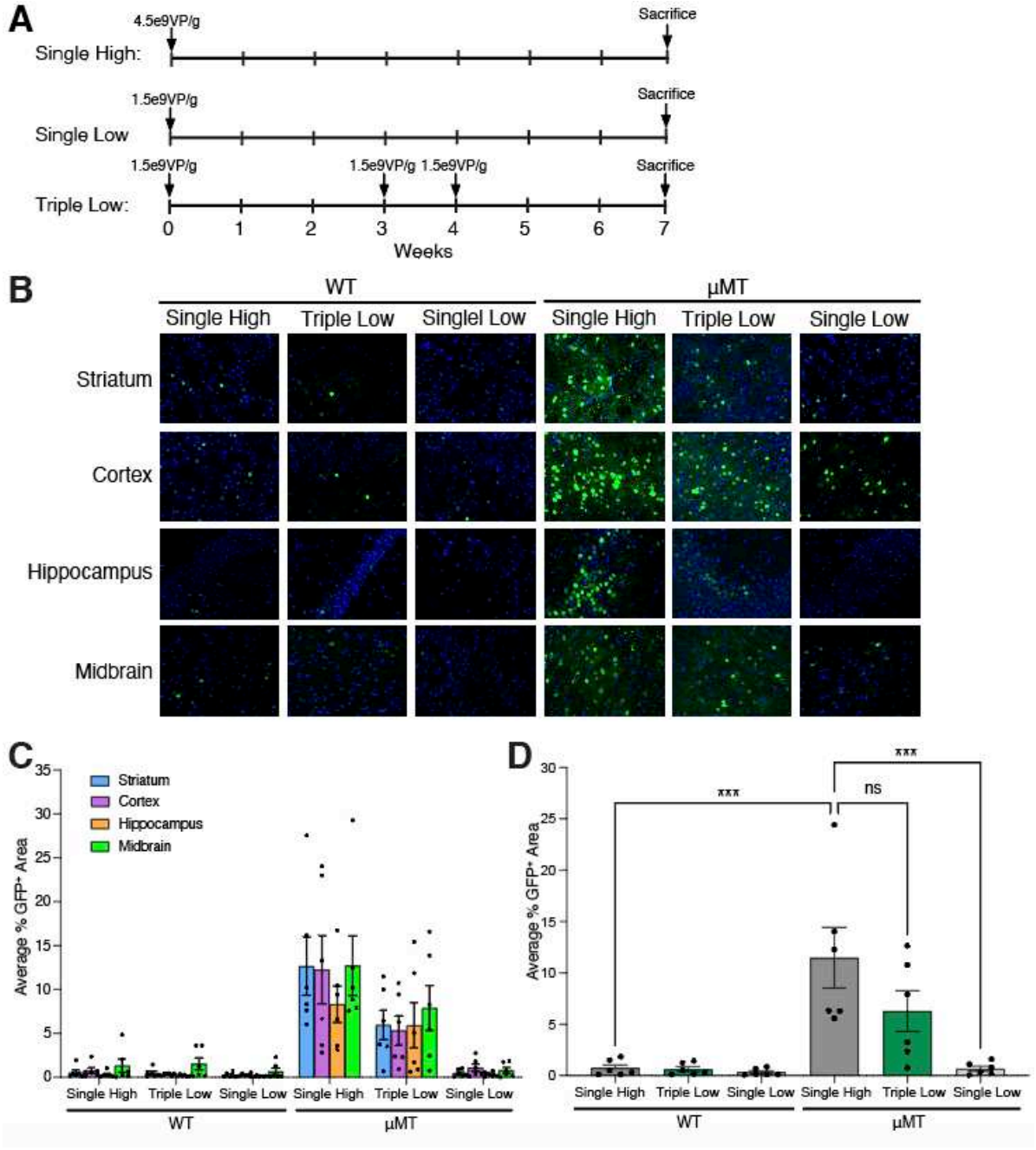

Fig 6. Re-administration of CAG-NLS-GFP PHP.eB to the brain. A, Timeline of re-administration studies (n=5 animals per group). µMT and WT mice were injected with a single high dose (4.5e9 VP/g), single low dose (1.5e9 VP/g), or three weekly repeated low doses (1.5e9 VP/g) of PHP.eB packaged with GFP driven by CAG promoter. **B**, Representative images of GFP expression in each brain region. **C**, Quantification of GFP expression by brain region defined as area above a threshold of 15 in ImageJ (N=5 animals per group). ns (not significant) not shown between regions in the same dose group, using 3-way ANOVA Tukey's testing. **D**, Average area GFP expression in the brain regions measured in **C**. *** indicates $P < 0.0002$ compared to other groups as measured by 2-way ANOVA with Tukey's post-hoc testing.

Supplementary Files

This is a list of supplementary files associated with this preprint. Click to download.

- SupplementaryInformationV1.pdf